

Review

Integrated Photonics on Glass: A Review of the Ion-Exchange Technology Achievements

Jean-Emmanuel Broquin ^{1,*} and Seppo Honkanen ²

¹ IMEP-LAHC, University Savoie Mont Blanc, University Grenoble Alpes, CNRS, Grenoble INP, 38000 Grenoble, France

² Institute of Photonics, University of Eastern Finland, 80100 Joensuu, Finland; seppo.honkanen@uef.fi

* Correspondence: jean-emmanuel.broquin@grenoble-inp.fr

Featured Application: ion-exchange on glass has been extensively studied for the realization of Planar Lightwave Circuits. Monolithically integrated on a single glass wafer, these devices have been successfully employed in optical communication systems as well as in sensing.

Abstract: Ion-exchange on glass is one of the major technological platforms that are available to manufacture low-cost, high performance Planar Lightwave Circuits (PLC). In this paper, the principle of ion-exchanged waveguide realization is presented. Then a review of the main achievements observed over the last 30 years will be given. The focus is first made on devices for telecommunications (passive and active ones) before the application of ion-exchanged waveguides to sensors is addressed.

Keywords: integrated photonics; glass photonics; optical sensors; waveguides; lasers



Citation: Broquin, J.-E.; Honkanen, S. Integrated Photonics on Glass: A Review of the Ion-Exchange Technology Achievements. *Appl. Sci.* **2021**, *11*, 4472. <https://doi.org/10.3390/app11104472>

Academic Editor:
Alessandro Belardini

Received: 25 April 2021
Accepted: 11 May 2021
Published: 14 May 2021

Publisher's Note: MDPI stays neutral with regard to jurisdictional claims in published maps and institutional affiliations.



Copyright: © 2021 by the authors. Licensee MDPI, Basel, Switzerland. This article is an open access article distributed under the terms and conditions of the Creative Commons Attribution (CC BY) license (<https://creativecommons.org/licenses/by/4.0/>).

1. Introduction

Unlike microelectronics where the CMOS technology emerged as the dominant platform, integrated optics or, as it is called nowadays, integrated photonics, does not rely on one single technological platform. Indeed, silicon photonics, III-V photonics, polymer photonics, LiNbO₃ photonics, and, last but not least, glass photonics co-exist in parallel, each of them presenting their own drawbacks and advantages.

As for ion-exchange on glass, also called glass integrated optics, it is based on a material that has been known and used for centuries. Glass is easily available and can be easily recycled. The ion-exchange technique, although it is based on using microfabrication tools, can be considered as a relatively low-cost approach, which allows realizing waveguides with low propagation losses and a high compatibility with optical fibers. Glass photonics is not a platform that has been developed for a specific application. Therefore, Planar Lightwave Circuits (PLCs) realized by ion-exchange on glass are found in many fields with a wide range of applications.

From its very beginning in 1972 [1], to products currently on the markets, thousands of papers have been published on this vivid topic. For this reason, making an extensive review of this technology is a cumbersome task. However, since excellent reviews have already been published in the past years [2–9], we can skip the pioneering years when the basis of the technology was set by testing several glasses and ions and making multimode waveguides. In this paper, we will hence focus on devices made by ion-exchange on glass, their performances, and their applications.

After a presentation of ion-exchanged waveguides, their realization process, their modelling, and their main characteristics, we will review devices made for telecommunication purpose. Then, we will review the use of ion-exchanged waveguides for the fabrication of optical sensors since these types of applications are taking a growing place in integrated photonics.

2. Ion-Exchanged Waveguides

2.1. Principle and Technology

Typically, an optical glass is an amorphous material composed by several types of oxides mixed together. According to Zachariassen [10], these oxides can be sorted in three main categories: network formers like SiO₂, GeO₂, or P₂O₅ that can create a glass on their own; intermediate network formers (Al₂O₃, TiO₂, . . .) that can hardly create a glass alone but can be combined with network formers; finally network modifier oxides like Na₂O, K₂O, CaO, or BaO that can be inserted in a matrix made by glass formers but are weakly linked to it because of a mismatch between their respective molecular binding structures.

The refractive index of a glass depends on its composition through an empirical relation [11]:

$$n = 1 + \sum_m \frac{a_m N_m}{V_0} = 1 + \frac{R_0}{V_0}, \quad (1)$$

where a_m is the “refractivity constant” of the chemical element “ m ”, N_m the number of chemical element “ m ” by atom of oxygen, V_0 and R_0 are the glass volume and refractivity by atom of oxygen, respectively.

A replacement of a portion of one of the glass components by another one with the same coordination can therefore entail a change of refractive index. Providing that this exchange does not create strong mechanical stresses and does not strongly change the nature of the glass, (1) can be used to link the induced variation of the refractive index to the fraction c of substituting ions as follows:

$$\Delta n = \frac{c}{V_0} \left(\Delta R - \frac{\Delta V R_0}{V_0} \right), \quad (2)$$

ΔR and ΔV are the variation of R_0 and V_0 , respectively, caused by the substitution. From (2), it can easily be deduced that a local change of the glass composition is creating a localized change of refractive index, which can be used to create a waveguide.

Since alkali ions are weakly linked to the glass matrix, they are natural candidates for such a process. Indeed, when alkali ions react with silica to form a multicomponent glass, the silica network is maintained because each silicon-oxygen tetrahedron remains linked to at least three other tetrahedra [12]. Therefore, one can exchange one alkali ion to another one without damaging the original glass. Throughout the years, several ion-exchanges have been demonstrated [13,14] but the topic of this article being integrated glass photonics, we will restrain ourselves on the few ones that have enabled realizing efficient devices. In this case, the ion that is present in the glass is usually Na⁺ (sometimes K⁺). It is nowadays mostly exchanged with silver (Ag⁺), more rarely with potassium (K⁺) or thallium (Tl⁺).

The ion source that allows creating the higher refractive index waveguide’s core can be either liquid or solid. The simplest way of performing an ion-exchange is described on Figure 1a. It consists in dipping the glass wafer in a molten salt containing a mixture of both the doping ions B⁺ and the glass ones A⁺. The salt is usually a nitrate, but sulfates are sometimes used when a temperature higher than 450 °C is required for the exchange. Although the principle of the process is very simple, it must be kept in mind that ionic diffusion is a process that strongly depends on the temperature; this parameter should hence be homogeneous all over the wafer and consequently in the molten salt. In order to define the parts of the wafer that will be ion-exchanged, a thin-film has previously been deposited and patterned in a clean room environment to define the diffusion apertures. Once the ion-exchange is completed, the masking layer is removed and diffused surface waveguides are obtained. If a more step-like refractive index profile is required, an electric field can be applied to push the doping ions inside the glass, as described in Figure 1b [1]. Nonetheless, this complicates the set-up and might also induce the reduction of the doping ions into metallic clusters that dramatically increase the propagation losses (specifically when silver is involved). The use of a silver thin film has also been employed successfully for the creation of the waveguide’s core [15]. The thin film can be either deposited on an

existing mask, as depicted on Figure 1c, or patterned directly on the glass substrate [16]. An applied electric field ensures an efficient electrolysis of Ag^+ ions into the glass by the consumption of the silver film anode. These three different processes allow realizing waveguides whose core is placed at the surface of the glass wafer and whose shape is, depending on the process parameters, semi-elliptical with a step refractive index change at their surface and diffused interfaces inside the glass. Intrinsically, such waveguides are supporting modes that are prone to interact with the elements present on the wafer surface. Interesting and even maximized for the realization of sensors, this interaction is often a drawback when dealing with telecom devices where the preservation of the quality of the optical signal is a key factor. For this reason, ion-exchanged waveguide cores are usually buried inside the glass.

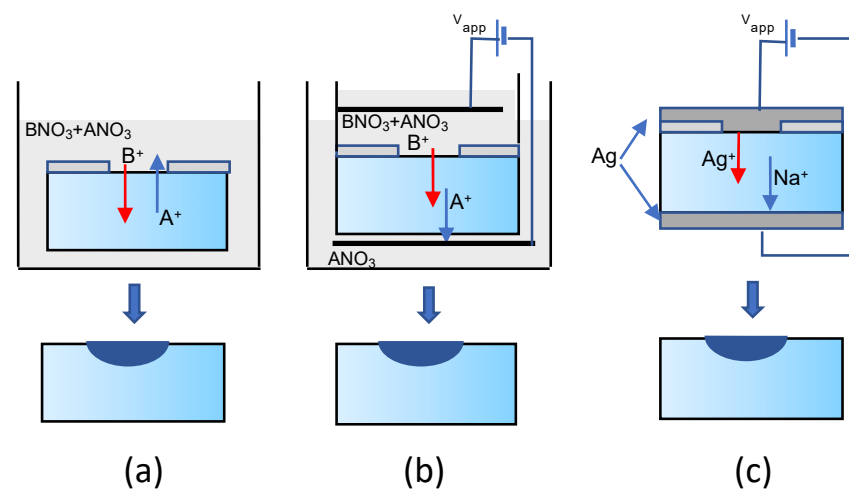


Figure 1. Three main processes used to realize surface waveguides by an ion-exchange on glass. A^+ and B^+ represent the ions contained in the glass and the ones replacing them, respectively. (a) the glass wafer is dipped into a molten salt containing B^+ ions entailing a thermal diffusion on the exchange ions through a diffusion aperture; (b) the diffusion process is assisted by an electric field; (c) an electrolysis of a silver thin film is used to generate Ag^+ ions that are migrating by diffusion and conduction inside the glass.

Figure 2 depicts the two main processes that can be used: the first one consists of plunging the wafer containing surface cores in a molten salt containing only the ions that were originally present in the glass. A reverse ion-exchange is then occurring, removing doping ions from the surface of the glass [17]. This process entails a quite important decrease of the refractive index change and an increase of the waveguide's dimension because of thermal diffusion, which practically limits the depth of the burying to one to two micrometers. In order to reach a deeper depth and ensure a good optical insulation of the guided mode, the reverse ion-exchange is quite often assisted by an electric field that forces the migration of the core inside the glass preventing hence a loss of refractive index variation. Moreover, by a proper tuning of the process parameters, circular waveguide cores can be obtained in order to maximize the coupling efficiency with optical fibers. Nonetheless, it must be noticed that the applied voltage can be close to 1 kV, which requires on one hand, a proper and well secured dedicated set-up, and on the other hand, an excellent quality of the glass wafer in order to prevent percolation path formation and short circuits. Figure 3 depicts an optical image of a buried optical waveguide realized on a Teem Photonics GO14 glass by a silver-sodium ion-exchange. Burying depth as high as $47\ \mu\text{m}$ have been realized, as shown in Figure 4, but such extreme values are rarely required in practical devices where the burying depth is of the order of $10\ \mu\text{m}$.

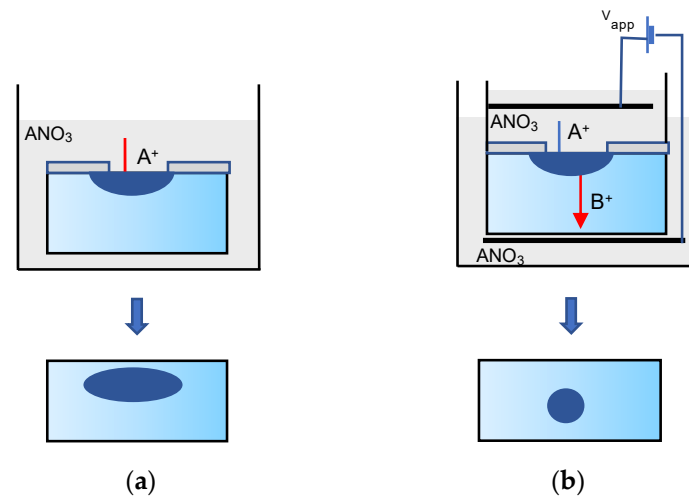


Figure 2. (a) Thermal burying of a waveguide's core; (b) electrically assisted burying of the waveguide's core. The competition between ionic diffusion and transport allows obtaining quasi circular profiles.

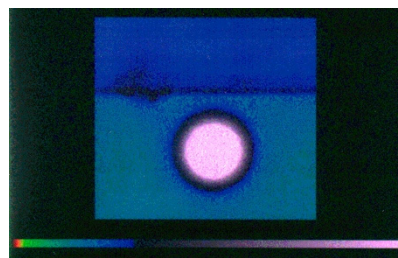


Figure 3. Image of a quasi-circular waveguide observed with an optical microscope, the glass is in light blue, the core is in pink, air is in dark blue.

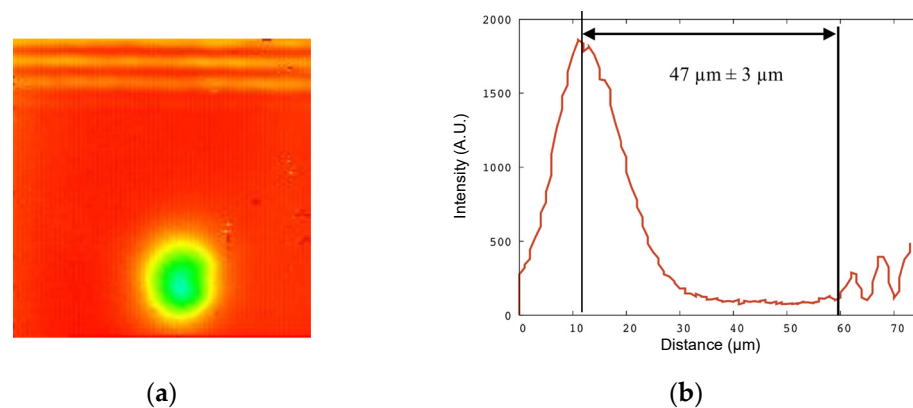


Figure 4. Realization of deeply buried waveguides by an Ag^+/Na^+ ion-exchange on a GO14 Teem-Photonics glass. The applied electric field during the burying process was 650 kV/m; (a) image of the output of the waveguide observed with an InGaAs Camera at $\lambda = 1.5 \mu\text{m}$; (b) vertical cut of the measured intensity showing the position of the mode with respect to the glass wafer substrate.

2.2. Modelling Ion-Exchanged Waveguides

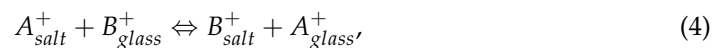
Extensive work has been carried-out throughout the years to characterize and model ion-exchanges processes [18–22]. In this article, we will focus on a relatively simple description since it occurred to be reliable enough to allow us designing waveguides and predicting their optical behavior efficiently. Ion-exchange can be seen as a two-step process: first the exchange itself that occurs at the surface of the glass and creates a normalized

concentration c_s of doping ions. For thin film sources, this concentration is linked to the applied current by the following relation:

$$\frac{\partial c_s}{\partial x} = \frac{J_0(c_s - 1)}{D_{Ag}}, \quad (3)$$

where J_0 is the ion flux created by the electrolysis, x is the direction normal to the surface, and D_{Ag} is the diffusion coefficient of silver in the glass.

For liquid sources made of a mixture of molten salts containing B^+ and A^+ ions in order to replace A^+ ions of the glass, an equilibrium at the glass surface is usually rapidly reached, according to the chemical reaction:



Considering that the amount of ions in the molten salt is much bigger than the one of the glass, the ion concentrations in the liquid source can be considered as constant, which allows deriving the relative concentration at the surface:

$$c_s = \frac{Kx_B}{1 + x_B(K - 1)}, \quad (5)$$

K being the equilibrium constant of the chemical reaction (4) and $x_B = C_B^{salt} / (C_B^{salt} + C_A^{salt})$ is the molar fraction of doping ions B^+ in the molten salt.

Since the refractive index is proportional to the relative concentration, according to (2), it is easy to fix the refractive index change at the glass surface by setting the ratio of B^+ ions in the liquid source. Figure 5 shows an experimental determination of this dependence for a silver/sodium ion-exchange on a Schott-BF33 glass. These data have been obtained by realizing highly multimode slab waveguides and retrieving their refractive index profile through m-lines measurements [23] and the Inv-WKB procedure [24,25].

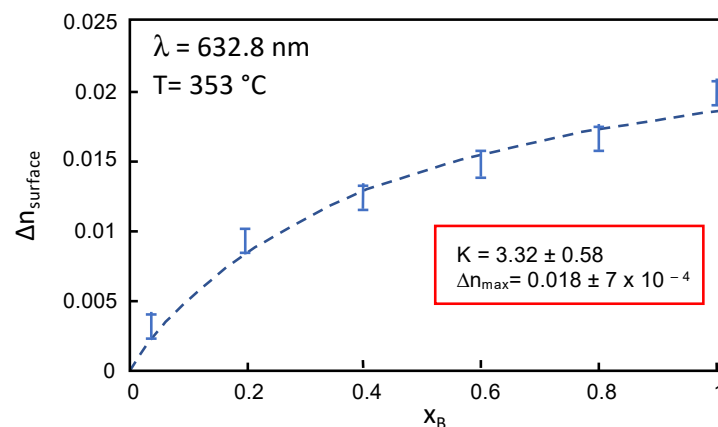


Figure 5. Refractive index change measured at the surface of a Schott-BF33 glass for different $x_B \text{AgNO}_3 + (1 - x_B) \text{NaNO}_3$ molten salts at a temperature of 353 °C.

The ions exchanged at the glass surface entail a gradient of concentration inside the glass. Hence, B^+ ions migrate inside the glass while A^+ ions are moving towards the surface. Since the two species of ions have different mobilities, an internal electrical field \vec{E}_{int} is created during the diffusion process. To this field an external applied field \vec{E}_{app} can

be added, which results in ions fluxes \vec{J}_A and \vec{J}_B , for A^+ and B^+ , respectively, which are determined by the Nernst–Einstein equation:

$$\begin{aligned} \vec{J}_A &= -D_A \left[\vec{\nabla} C_A - \frac{e}{H k_B T} C_A (\vec{E}_{int} + \vec{E}_{app}) \right] \\ \vec{J}_B &= -D_B \left[\vec{\nabla} C_B - \frac{e}{H k_B T} C_B (\vec{E}_{int} + \vec{E}_{app}) \right], \end{aligned} \tag{6}$$

where D_i is the diffusion coefficient of the ion i , C_i its concentration, e is the electron charge, k_B the Boltzmann constant, T the temperature and H the Haven coefficient. Assuming that all the sites left by ions A^+ are filled by ions B^+ , it can be written that at any position in the glass the relation $C_A + C_B = C_{A0}$, where C_{A0} is the concentration of A^+ ions before the exchange, is always valid. With this relation and Equation (6), the total ionic flux can be expressed as:

$$\vec{J} = \vec{J}_A + \vec{J}_B = -D_A C_{A0} \left[\alpha \vec{\nabla} c - \frac{e}{H k_B T} (1 - \alpha c) (\vec{E}_{int} + \vec{E}_{app}) \right], \tag{7}$$

where the Steward coefficient $\alpha = 1 - D_B/D_A$ and the normalized concentration $c = C_B/C_{A0}$ have been introduced.

If no electric field is applied, then the total current is null, which allows determining easily \vec{E}_{int} :

$$\vec{E}_{int} = - \frac{H k_B T}{e} \frac{\alpha \vec{\nabla} c}{1 - \alpha c} \tag{8}$$

The second Fick’s law implies that:

$$\frac{\partial C_B}{\partial t} = -\nabla \cdot \vec{J}_B. \tag{9}$$

Combining (6), (8) and (9), the equation that governs the evolution of the relative concentration as a function of time is obtained:

$$\frac{\partial c}{\partial t} = \vec{\nabla} \cdot \left[\frac{D_B}{1 - \alpha c} \vec{\nabla} c - \frac{e D_B}{H k_B T} c \vec{E}_{app} \right]. \tag{10}$$

Equation (10) can be solved numerically by Finite Difference or Finite Element schemes but for accurate modelling, the dependence of ionic mobility and diffusion on the concentration should not be neglected. The so-called mixed alkali effect plays indeed a significant role in ion-exchanges where a high doping concentration is required [26,27]. It must also be noticed that ion-exchange modifies the conductivity of the glass, which in turn, modifies the field distribution of \vec{E}_{app} . Therefore, solving Equation (10) is actually much less obvious than it might appear and handling these problems has been the subject of a quite abundant literature [28–31]. Figure 6 displays typical refractive index profiles that have been obtained considering mixed alkali effect and the coupling between the ion-exchange and the applied electric field. Simulations have been done with an in-house software based on a finite difference scheme. It can be clearly seen how a proper choice of the experimental parameters can lead to circular waveguides. However, the maximum refractive index change is dropping from almost 0.1 to 10^{-2} during the burial process because of the spreading of doping ions caused by thermal diffusion.

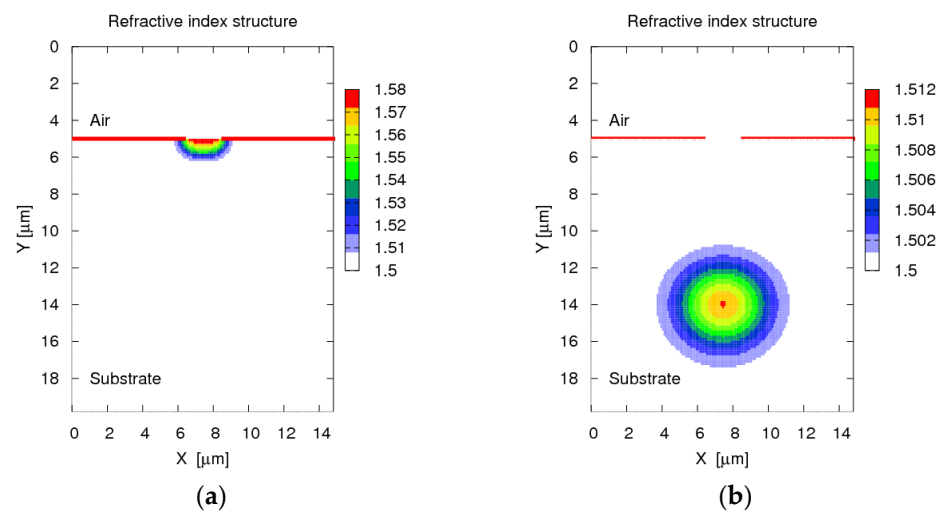


Figure 6. (a) Refractive index distribution of a thermally diffused waveguide, diffusion aperture width is 2 μm , exchange time is 2 min, $D_B = 0.8 \mu\text{m}^2/\text{min}$; (b) refractive index profile of the waveguide (a) after an electrically assisted burying in a pure NaNO_3 molten salt, process duration is 1 h30 for an applied electric field of 180 kV/m.

2.3. Waveguide's Performances

The main characteristics when dealing with integrated optics waveguides are their spectral operation range, their losses that can be split between coupling and propagation losses, and their behavior with respect to light polarization.

2.3.1. Passive Glasses

Since the first waveguides demonstrated by Izawa and Nakagome [1], huge efforts have been made to reduce the losses of the waveguides. Historically, scattering represented the main source of losses. Indeed, the quality of the photolithography used for the realization of the masking layer before the ion-exchange was an issue as well as scratches or dirt deposited on the glass surface or refractive index inhomogeneities, such as bubbles. These problems are typical optical glass issues that are encountered when a custom-made glass is realized for the first time in small volumes, but they are easily handled by glass manufacturers when a higher volume of glass is produced. Therefore, state-of-the-art ion-exchanged waveguides are nowadays based on glass wafers specifically developed for this application or at least for microtechnologies. Among them, the more used are BF33 by Schott because of its compatibility with MEMS process, GO14 by TeemPhotonics SA and BGG31 by Schott [32], which have both been developed specifically for silver-sodium ion-exchanges. The interest of silver-sodium ion-exchange is that it allows the realization of buried waveguides solving, hence the problem of scattering due to surface defects or contaminations while dramatically improving the coupling efficiency with optical fibers. Nonetheless, silver-based technologies present also challenges since Ag^+ has a strong tendency to reduce into metallic Ag creating metallic clusters that are absorbing the optical signals. The glass composition should therefore be adapted not only to remove reducing elements like Fe, As, or Sb, but also to create a glass matrix where Na^+ ions are not linked to non-bridging oxygens [33]. The choice of the material for the masking layer should also be made with caution because the use of metallic mask can also induce the formation of Ag nanoparticles at the vicinity of the diffusion apertures [34]. Therefore, the use of Al or Ti mask is now often replaced by Al_2O_3 [35,36], SiO_2 , or SiN [37] ones.

Table 1 presents the main characteristics of single mode waveguides realized on GO14, BGG31, and BF33, respectively. GO14 and BGG31 that have been optimized for telecom applications and ion-exchange present very low propagation losses and birefringence that are key characteristics for data transmission. BF33 is not a glass that has been designed for ion-exchange but it is a relatively low-cost glass that presents a quite good refractive index

change and that is specifically indicated by its manufacturer for MEMS and microtechnology applications. Therefore, it is an excellent candidate for sensor realization and is mainly used for that. The relatively high propagation losses observed in BF33 is mainly due to the fact that this parameter is not very important in sensors and has, hence, neither been optimized nor measured accurately.

Table 1. Main characteristics of single mode waveguides realized on three different glasses.

Glass Type	GO14	BGG31	BF33
Losses	<0.05 dB/cm [7]	<0.1 dB/cm	<1 dB/cm (@780 nm)
Δn max	8×10^{-2} [7]	3.2×10^{-2} [38]	1.8×10^{-2} [35]
Birefringence	$<5 \times 10^{-4}$ [39]	$<2 \times 10^{-5}$ [40]	N.A.
Burying depth	$\sim 10 \mu\text{m}$ (50 μm max)	$\sim 10 \mu\text{m}$ [38]	$\sim 5 \mu\text{m}$ [35]

We deliberately did not mention Tl^+/K^+ ion-exchanged waveguides although the process is indeed the first one that has been used and the first one to be tentatively implemented in a production line. However, the advantages of a Tl^+/K^+ ion-exchange, namely a high refractive index change and the absence of clustering and absorption, are strongly counterbalanced by its toxicity, which implies dedicated safety procedures and waste treatments. It is therefore very scarcely used.

2.3.2. Active Glasses

The possibility of performing ion-exchange on rare-earth doped glasses was identified quite early. However, it was only in the 1990s with the development of WDM telecommunication that a lot of work was carried-out on the realization of efficient optical amplifiers and lasers. Because the solubility of rare earths into silicate glasses is quite low, which entails quenching due to clustering and reduces the amplifier efficiency, phosphate glasses rapidly emerged as the most efficient solution for obtaining high gain with compact devices. Among phosphate glasses, two specific references set the state of the art: they were the IOG 1 by Schott [41] and a proprietary glass referred as P1 by TeemPhotonics [42]. These two glasses succeeded in obtaining a high doping level without rare-earth clustering while being chemically resistant enough to withstand clean room processes and ion-exchange. The competition in the field of rare earth doped waveguides having been very hard, the characteristics of the different waveguides obtained in these glasses are difficult to find in the literature since the emphasis was mostly put on the active device performances, as will be detailed later.

2.3.3. Exotic Substrates

Some exotic glasses like fluoride glasses [43] or germanate glasses [44,45] have also been used for the realization of ion-exchanged waveguides but the difficulty in making sufficiently good wafers available at a reasonable cost, strongly limited the research in these directions.

3. Telecom Devices

3.1. Context and Historical Overview

Optical Telecommunications was originally the reason why Miller introduced the concept of integrated optics in 1969 [46]. Therefore, the pioneering work of integrated photonics on glass has been mainly devoted to telecommunication devices pushing steadily towards the development of not only ion-exchange processes but also of a full technology starting from the wafer fabrication and ending with the packaging of the manufactured Planar Lightwave Circuits. Figure 7 shows this evolution by displaying on one side one of the first demonstrations of a 1 to 8 power splitter made by cascading multimode Y-junctions [47] and, on the other side, its 2006 commercially available counterpart, single mode and Telcordia 1209 and 1221 compliant [7,48].

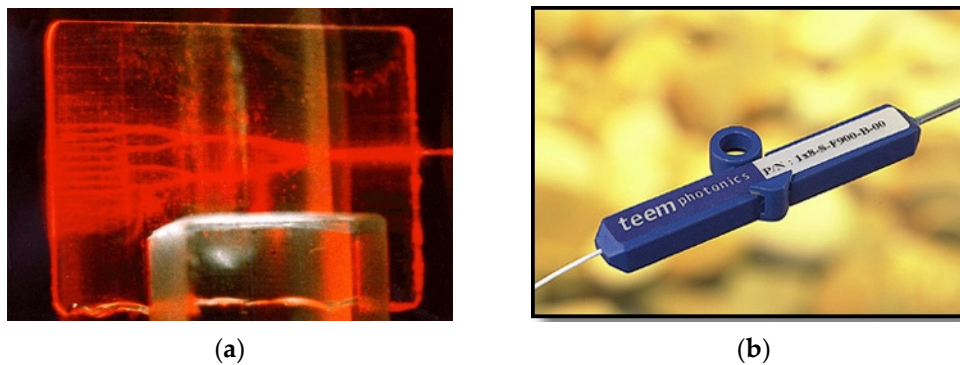


Figure 7. 1 to 8 power splitter made by ion-exchange on glass (a) early demonstration in 1986; (b) qualified pigtailed and packaged commercially available product.

Once elementary functions, such as Y-junctions and directional couplers were demonstrated, studies were oriented towards all the functions that could be required for optical fiber communications like thermo-optic switches [49], Mach–Zehnder interferometers [50,51] and Multimode Mode Interference (MMI) couplers [52–55]. These building blocks have then been optimized and/or combined on a single chip to provide more functionality. In the next sections, we will review some of them and put the emphasis on the specificity brought by the use of ion-exchange on glass.

3.2. Wavelength Multiplexers

A five-channel wavelength demultiplexer-multiplexer has been demonstrated as early as 1982 by Suhara et al. using silver multimode waveguides combined with a Bragg grating [56]. More advanced devices using single mode waveguides include Arrayed-Waveguide Grating (AWG) multiplexers, whose quite large footprint is compensated by their low sensitivity to the light polarization thanks to the use of silver based buried waveguides [38]. A good thermal stability provided by the thickness of the glass substrate is also reported but a fine thermal tuning of the AWG's response remained possible [57]. Add and drop multiplexing has been achieved by combining Bragg gratings with Mach–Zehnder interferometers or more originally with a bimodal waveguide sandwiched by two asymmetric Y-branches [58]. Bragg grating can be integrated on glass by etching [59], wafer bonding [60], or photowriting [61–63].

Asymmetric Y-junctions are very interesting adiabatic devices that are well adapted to the smooth transitions between waveguides obtained by ion-exchange processes. Therefore, asymmetric Y-junctions have been used as stand-alone broadband wavelength multiplexers. For this type of applications, the asymmetry of the branches is obtained by a difference of the waveguide dimensions and a difference in their refractive index. Tailoring the refractive index of ion-exchanged waveguides can be achieved by segmenting the waveguide as demonstrated by Bucci et al. [64]. As can be seen on Figure 8, using vertical integration of deeply buried waveguides with selectively buried waveguides allowed obtaining a very broadband duplexing behavior while maintaining a relatively small surface footprint [36].

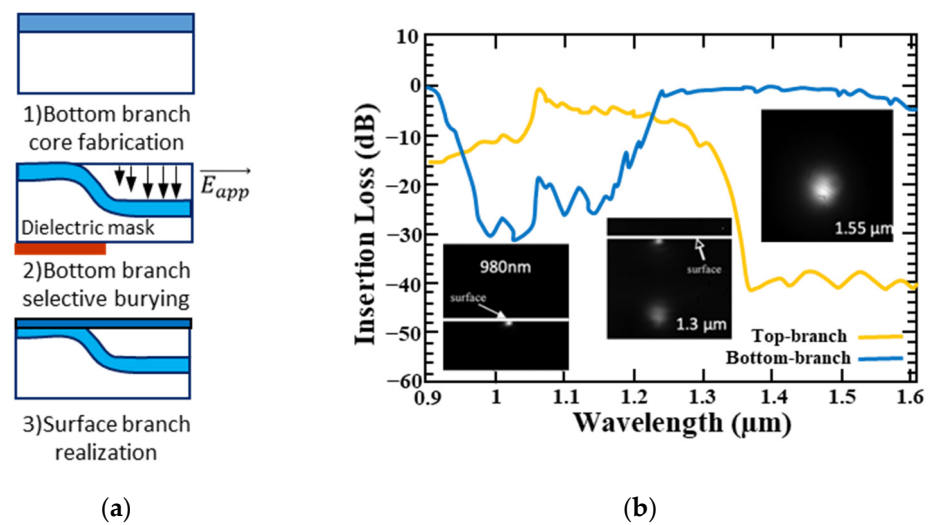


Figure 8. Vertically integrated broadband duplexer (a) fabrication steps; (b) measured transmission (the insets display the observed device output's mode at specific wavelengths). Top and bottom branches are separated by $28 \mu\text{m}$ [36].

3.3. Waveguide Amplifiers and Lasers

Active devices have been linked to the development of ion-exchanged devices since the beginning of this technology. Indeed, Saruwatari et al. demonstrated in 1973 a laser made with an optical amplifier based on a buried multimode ion-exchanged waveguide realized in a neodymium-doped borosilicate glass [65]. However, research on active devices really became a major field of research with a strong competition at the beginning of the 1990s when a lot of studies were carried-out. Work was first concentrated on Nd-doped amplifiers and lasers emitting at $1.06 \mu\text{m}$ since the four energy levels pumping scheme of this transition made it easier to achieve a net gain with the 800 nm pumping diodes available at the moment [66–70]. With the rise of Wavelength Division Multiplexing systems, optical amplifiers and sources operating in the C+L band (from 1525 nm to 1610 nm) became key devices and research on rare-earth doped integrated devices switched to the use of erbium ions whose transitions from the ${}^4I_{13/2}$ level to the ${}^4I_{15/2}$ one is broad enough to cover this wavelength range. Dealing with Er^{3+} active ions, the main issue was to realize waveguides with low-losses and a good overlap of the pump and signal modes. Indeed, the pumping scheme of this rare earth being a three levels one, the ${}^4I_{15/2}$ ground state absorbs the optical signal when it is not sufficiently pumped. Barbier et al. managed to solve this problem by developing a silver-sodium ion-exchange in their Er/Yb co-doped P1 glass [42]. 41 mm-long buried waveguides achieved 7 dB of net gain in a double pass configuration. This work has been followed by the demonstration of an amplifying four wavelength combiner [71] and the qualification of Erbium Doped Waveguide Amplifiers (EDWAs) in a 160 km-long WDM metro network [72]. This work has been completed by packaging and qualification developments in order to create a product line commercialized by TeemPhotonics.

Meanwhile the phosphate glasses developed by Schott also gained a lot of attention. Patel et al. achieved a record high gain of 13.7 dB/cm in a 3 mm-long waveguide realized by a silver film ion-exchange [73]. Such a gain per length unit was made possible by a high doping level of the glass in Er (8 wt. %) and Yb (12 wt. %).

Er-doped waveguide amplifiers being available, Er-doped lasers followed. Actually, the first proof of concept of an ion-exchanged waveguide laser was obtained on a modified BK7-silicate glass containing 0.5 wt. % of Er, with a potassium ion-exchange and two thin-film dielectric mirrors bonded to the waveguide's facets forming a Fabry-Perot cavity [74]. Nonetheless, from a strict point of view, this device was not a fully integrated laser because the mirrors were not integrated on the chip. Therefore, the next generation of Er-laser relied on the use of Bragg gratings as mirrors. In Distributed FeedBack (DFB) or Distribute Bragg

Reflectors configurations, these lasers presented a single frequency emission compatible with their use as transmitters in WDM systems. Similar for waveguide amplifiers, the use of phosphate glass entailed a major breakthrough in the performances. DBR lasers were demonstrated by Veasey et al. using a potassium ion-exchange [41], while Madasamy et al. manufactured similar devices with a silver thin film [75]. These approaches allowed integrating several lasers on a single chip to provide arrays of multiwavelength sources with one single grating, the wavelength selection being made by tuning the effective indices of the waveguides through their dimensions. Thanks to the use of highly concentrated molten salt of silver nitrate and a DFB configuration, Blaize et al. succeeded in creating a comb of 15 lasers with one single Bragg grating [76]. The emitters' wavelengths were spaced by 25 GHz and 100 GHz and set to be on the Dense WDM International Telecommunication Union (ITU) grid. The output power of these devices could be as high as 80 mW for a 350 mW coupled pump power [41], while a linewidth of only 3 kHz has been reported by Bastard et al. on their DFB lasers [77]. Figure 9 displays a picture of such a DFB laser pigtailed to HI1060 single mode fibers. The stability and purity of the emission of erbium doped waveguide lasers has been recently used to generate a Radio Frequency signal and successfully transmit data at a frequency of 60 GHz [78].

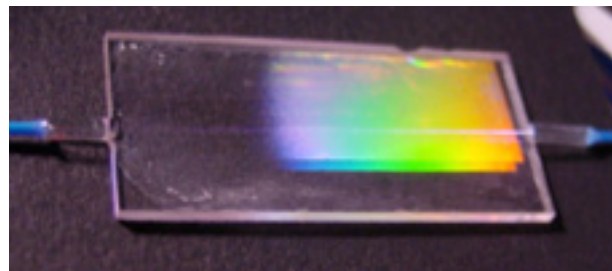


Figure 9. Picture of a DFB laser realized by silver-sodium ion-exchange on P1 phosphate glass at the IMEP-LaHC (device similar to [77]).

Bragg gratings on phosphate glass can be made by photolithography steps and etching like in [41,76,77] or by direct UV inscription like in [79,80] and on IOG1. The use of a hybrid un-doped/doped IOG1 substrate allowed Yliniemi et al. [80] to realize UV-written Bragg gratings with high reflectance and selectivity, demonstrating hence a single frequency emission with an output power of 9 mW and a slope efficiency of 13.9%.

3.4. Hybrid Devices

Ion-exchanged waveguides being made inside the glass wafer, they leave its surface plane and available for the integration of other materials or technologies. The realization of deeply buried waveguides [81] and selectively buried waveguides [82] acting as optical vias between two different layers increased furthermore the possibility of 3D integration. In order to overcome the quite weak chemical durability of an Yb-Er doped phosphate glass, Gardillou et al. [83] wafer bonded it on a silicate glass substrate containing surface Tl ion-exchanged strips. The higher refractive index active glass was then thinned by an appropriate polishing process to become a single mode planar waveguide. At the place where the planar waveguide was in contact with the ion-exchanged strips, the variation of refractive index provided the lateral confinement creating hence a hybrid waveguide. A gain of 4.25 dB/cm has been measured with this device. This approach has been pursued by Casale et al. [59] who realized a hybrid DFB laser combining a planar ion-exchanged waveguide made on IOG1 with a passive ion-exchanged channel waveguide realized on GO14. The Bragg grating was etched on the passive glass and encapsulated between the two wafers.

Polymers have also been used to functionalize an ion-exchanged waveguide. As an example, a thin film of BDN-doped cellulose acetate deposited on the surface of ion-exchanged waveguide lasers allowed the realization of passively Q-switched lasers on

Nd-doped [84] and Yb doped [85] IOG1 substrates. A peak power of 1 kW for pulses of 1.3 ns and a repetition rate of 28 kHz has been reported by Charlet et al. [86] and used successfully to pump a photonic crystal fiber and generate a supercontinuum [87].

Recently, a proof of concept of LiNbO₃ thin films hybridized on ion-exchanged waveguides have been reported [88]. The combination of these two well-known technological platforms for integrated photonics opens the route towards efficient low-loss non-linear integrated devices including electro-optic modulators.

Hybrid integration of semiconductor devices on glass wafers containing ion-exchanged waveguides have been reported for the first time in 1987, by MacDonald et al. [89] They bonded GaAs photodiodes on a metallic layer previously deposited and patterned on the glass wafer. Waveguides were done by a silver thin film dry process. Silicon [90] and germanium [91] photodetectors have been produced on potassium waveguides, while Yi-Yan et al. proposed a lift-off approach to bond thin III-V semiconductor membranes on the surface of a glass wafer containing ion-exchanged waveguide and realize Metal–Semiconductor–Metal (MSM) photodetectors [92].

4. Sensors

Integrated photonics is intrinsically interesting for the realization of optical sensors because it provides compact and reliable self-aligned devices that can be easily deployed when pigtailed to optical fibers. Glass is a material that is chemically inert, bio-compatible, and mechanically stable. Therefore, making optical sensors on glass wafers or integrating optical glass chips into complex set-ups have encountered a huge interest. We will detail here a selection of ion-exchanged based glass sensors as examples of possible applications.

Although AWGs used in telecom are actually integrated spectrometers, they are not well adapted to the rapid measurement of full spectra. For this reason, a Stationary-Wave Integrated Fourier-Transform Spectrometer (SWIFTS) has been proposed and developed [93]. It is a static Fourier Spectrometer that measures directly the intensity of a standing wave with nanoprobe placed on a waveguide. In the instrument reported by Thomas et al. [94], the waveguide is made by a silver ion-exchange on a silicate glass and the nanoprobe is a gold nanodot. The interaction of gold nano-antennas with an ion-exchanged waveguide has been studied by Arnaud et al. [95]. This spectrometer has a spectral measurement range that starts at 630 nm and ends at 1080 nm with a spectral resolution better than 14 pm. SWIFTS interferometers are currently integrated in the product line commercialized by Resolution Spectra Systems [96].

Displacement sensors allow measuring accurately the change of position of an object through interferometry. Helleso et al. [97] implemented a double Michelson interferometer on a glass substrate using potassium ion-exchange; the device provided two de-phased outputs in order to give access not only to the distance of the displacement but also its direction. However, having only two interferometric signals is not sufficient to prevent the measure from being affected by unexpected signal variations. For this reason, Lang et al. [98] proposed a new design for the interferometric head that provided four quadrature phase shifted outputs. The device made by potassium ion-exchange demonstrated a measurement accuracy of 79 nm over a measurement range of several meters when used with an HeNe laser as a source. After technological improvements and the use of a silver-sodium ion-exchange on GO14 glass, an evolution of this sensor is now commercialized by TeemPhotonics and presents a resolution of 10 pm for a 1530 nm–1560 nm operating wavelength range [48].

Measuring speed is also something that can be of major importance, specifically in the case of aircrafts where their True Air Speed (TAS), which is their speed with respect to the air surrounding them, conditions their lift. Airborne LIDARs have hence been developed as a backup to Pitot gauges in order to increase the safety of flight by providing a redundant accurate measurement of the aircraft TAS. The operation principle of an airborne LIDAR is based on the Doppler frequency shift measured on a laser signal reflected on the dust particles of the atmosphere. This shift being quite low and presenting a low amplitude

when compared to the emitted signal, a laser source that presents a narrow linewidth, a low Relative Intensity Noise and that is resilient to mechanical vibrations is required. Bastard et al. [99] realized such a laser source on an Er/Yb doped phosphate glass with silver ion-exchanged waveguides and a DFB structure. This laser presented a fiber coupled output power of 2.5 mW, a linewidth of 2.5 kHz, and a RIN that was 6 dB lower than the specification limit. The device has then been successfully implemented in the LIDAR set-up and validated in flight [100].

Astrophysical research programs rely on telescopes with always higher resolution to detect exoplanets, young star accretion disks, etc. Optical long baseline instruments, which interferometrically combine the signal collected by different telescope have been developed for this purpose. Such complex interferometers are very sensitive to misalignment and vibrations, therefore the use of integrated optics as telescope recombiners have been studied. Haguenaer et al. [101] used a silver-sodium ion-exchange on a silicate glass to realize a two telescope beam combiner operating on the H atmospheric band (from $\lambda = 1.43 \mu\text{m}$ to $\lambda = 1.77 \mu\text{m}$). Consisting of a proper arrangement of three Y-junctions, the device had two photometric and one interferometric outputs. The fringe contrast obtained in the laboratory was 92% and the device was included in the Integrated Optic Near infrared Interferometric Camera (IONIC) put into a cryostat and successfully qualified on the sky [102]. Figure 10 shows the MAFL chip [103] that was developed for the interferometric combination of three telescopes. The pigtailed instrument contained not only the science interferometers but also three other ones dedicated to metrology, which permitted measuring of the different optical paths. The functions multiplexing and demultiplexing the metrology signal and the science ones were also implemented on the chip.

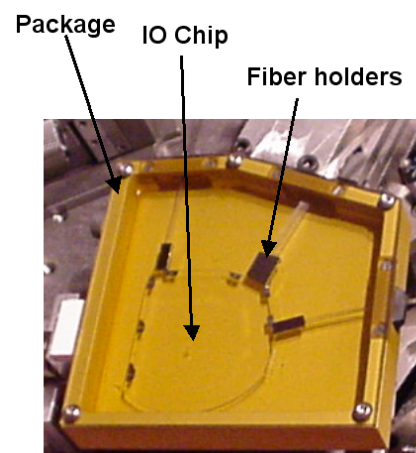


Figure 10. Picture of the MAFL combining module. The optical chip contains waveguides made by a silver sodium ion-exchange.

The chemical durability of silicate glasses is a major advantage when a use in harsh environment is required. The opto-fluidic sensor developed by Allenet et al. [104] represents a quite extreme example of this. Indeed, the ion-exchange technology developed by Schimpf et al. [35] on BF33 glass has been employed to realize a sensor for the detection of plutonium in a nuclear plant environment. The fully pigtailed and packaged device that is depicted on Figure 11, has been successfully tested in a nuclearized glove box, detecting plutonium dissolved in 2 Mol nitric acid without a failure over a period of one month. Such a reliability was achieved by co-integrating microfluidic channels fabricated by HF wet etching on one BF33 wafer with silver ion-exchanged waveguides realized on another wafer. The two wafers have been assembled by molecular adherence avoiding hence the use of radiation sensitive epoxy glues.

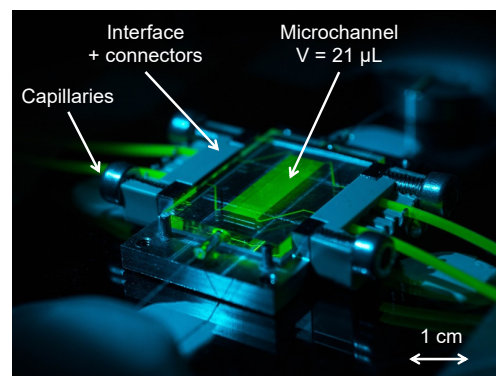


Figure 11. Picture of an optofluidic sensor realized on BF33 glass wafer for the measurement of radioactive elements diluted in highly concentrated nitric acid.

5. Conclusions

In this paper, we reviewed over thirty years of activities in glass photonics. The ion-exchange realization process as well as its modelling has been exposed. Passive and active devices for telecommunication applications have then been presented with the emphasis on the major breakthroughs of this field. The section dedicated to sensors underlines the evolution of the ion-exchange technology, which is moving from quite simple, though extremely performant functions, to more complex integrated optical microsystems. The authors hope that the picture of glass photonics that they presented will soon be outdated by the new results that are currently being elaborated in the many laboratories of universities and companies involved in this field throughout the world.

Funding: The visit of Pr Broquin at the University of Eastern Finland is funded by the Nokia Foundation within the frame of the Institut Français de Finlande—Nokia Foundation Distinguished Chair. This work is also part of the Academy of Finland Flagship Programme, Photonics Research and Innovation (PREIN), decision 320166.

Institutional Review Board Statement: Not applicable.

Informed Consent Statement: Not applicable.

Conflicts of Interest: The authors declare no conflict of interest.

References

- Izawa, T. Optical waveguide formed by electrically induced migration of ions in glass plates. *Appl. Phys. Lett.* **1972**, *21*, 584–586. [[CrossRef](#)]
- Terai, R.; Hayami, R. Ionic diffusion in glasses. *J. Non-Crystalline Solids* **1975**, *18*, 217–264. [[CrossRef](#)]
- Findakly, T. Glass Waveguides by Ion Exchange: A Review. *Opt. Eng.* **1985**, *24*, 242244. [[CrossRef](#)]
- Ramaswamy, R.; Srivastava, R. Ion-exchanged glass waveguides: A review. *J. Light. Technol.* **1988**, *6*, 984–1000. [[CrossRef](#)]
- Ross, L. Integrated Optical Components in Substrate Glasses. *Glastech. Ber.* **1989**, *62*, 285–297.
- Nikonorov, G.T.; Petrovskii, N.V. Ion-exchanged glasses in integrated optics: The current state of research and prospects (a review). *Glass Phys. Chem.* **1999**, *25*, 16–55.
- Broquin, J.E. Glass integrated optics: State of the art and position toward other technologies. In Proceedings of the Integrated Optics: Devices, Materials, and Technologies XI, San Jose, CA, USA, 22–24 January 2007.
- Mazzoldi, P.; Sada, C. A trip in the history and evolution of ion-exchange process. *Mater. Sci. Eng. B* **2008**, *149*, 112–117. [[CrossRef](#)]
- West, B.R.; Tervonen, A.; Honkanen, S. Ion-exchanged glass waveguide technology: A review. *Opt. Eng.* **2011**, *50*, 071107. [[CrossRef](#)]
- Zachariasen, W.H. The atomic arrangement in glass. *J. Am. Chem. Soc.* **1932**, *54*, 3841–3851. [[CrossRef](#)]
- Huggins, M.L.; Sun, K.H.; Davis, D.O. The Dispersion of Silicate Glasses as a Function of Composition II*. *J. Opt. Soc. Am.* **1942**, *32*, 635–648. [[CrossRef](#)]
- Doremus, R.H. *Glass Science*; Wiley & Sons: New York, NY, USA, 1973.
- Lilienhof, H.J.; Voges, E.; Ritter, D.; Panschew, B. Field-induced index profiles of multimode ion-exchanged strip waveguides. *IEEE J. Quantum Electron.* **1982**, *18*, 1877–1883. [[CrossRef](#)]
- Chartier, G.; Jaussaud, P.; De Oliveira, A.; Parriaux, O. Fast fabrication method for thick and highly multimode optical waveguides. *Electron. Lett.* **1977**, *13*, 763–764. [[CrossRef](#)]

15. Viljanen, J.; Leppihalme, M. Fabrication of optical strip waveguides with nearly circular cross section by silver ion migration technique. *J. Appl. Phys.* **1980**, *51*, 3563–3565. [[CrossRef](#)]
16. Pantchev, B. One-step field-assisted ion exchange for fabrication of buried multimode optical strip waveguides. *Electron. Lett.* **1987**, *23*, 1188–1190. [[CrossRef](#)]
17. Seki, M.; Hashizume, H.; Sugawara, R. Two-step purely thermal ion-exchange technique for single-mode waveguide devices in glass. *Electron. Lett.* **1988**, *24*, 1258–1259. [[CrossRef](#)]
18. Prieto-Blanco, X. Electro-diffusion equations of monovalent cations in glass under charge neutrality approximation for optical waveguide fabrication. *Opt. Mater.* **2008**, *31*, 418–428. [[CrossRef](#)]
19. Quaranta, A.; Cattaruzza, E.; Gonella, F. Modelling the ion exchange process in glass: Phenomenological approaches and perspectives. *Mater. Sci. Eng. B* **2008**, *149*, 133–139. [[CrossRef](#)]
20. Quaranta, A.; Rahman, A.; Mariotto, G.; Maurizio, C.; Trave, E.; Gonella, F.; Cattaruzza, E.; Gibaudo, E.; Broquin, J.E. Spectroscopic Investigation of Structural Rearrangements in Silver Ion-Exchanged Silicate Glasses. *J. Phys. Chem. C* **2012**, *116*, 3757–3764. [[CrossRef](#)]
21. Albert, J.; Lit, J.W. Full modeling of field-assisted ion exchange for graded index buried channel optical waveguides. *Appl. Opt.* **1990**, *29*, 2798–2804. [[CrossRef](#)] [[PubMed](#)]
22. Tervonen, A. A general model for fabrication processes of channel waveguides by ion exchange. *J. Appl. Phys.* **1990**, *67*, 2746–2752. [[CrossRef](#)]
23. Tien, P.K.; Ulrich, R. Theory of Prism–Film Coupler and Thin-Film Light Guides. *J. Opt. Soc. Am.* **1970**, *60*, 1325–1337. [[CrossRef](#)]
24. Chiang, K. Construction of refractive-index profiles of planar dielectric waveguides from the distribution of effective indexes. *J. Light. Technol.* **1985**, *3*, 385–391. [[CrossRef](#)]
25. White, J.M.; Heidrich, P.F. Optical waveguide refractive index profiles determined from measurement of mode indices: A simple analysis. *Appl. Opt.* **1976**, *15*, 151–155. [[CrossRef](#)] [[PubMed](#)]
26. Kirchheim, R.; Paulmann, D. The relevance of site energy distribution for the mixed alkali effect. *J. Non-Cryst. Solids* **2001**, *286*, 210–223. [[CrossRef](#)]
27. Lupascu, A.; Kevorkian, A.; Boudet, T.; Saint-Andre, F.; Persegol, D.; Levy, M. Modeling ion exchange in glass with concentration-dependent diffusion coefficients and mobilities. *Opt. Eng.* **1996**, *35*, 1603–1610. [[CrossRef](#)]
28. West, B.R.; Madasamy, P.; Peyghambarian, N.; Honkanen, S. Modeling of ion-exchanged glass waveguide structures. *J. Non-Cryst. Solids* **2004**, *347*, 18–26. [[CrossRef](#)]
29. Hazart, J.; Minier, V. Concentration profile calculation for buried ion-exchanged channel waveguides in glass using explicit space-charge analysis. *IEEE J. Quantum Electron.* **2001**, *37*, 606–612. [[CrossRef](#)]
30. Masalkar, P.J. Calculation of Concentration Profile in Ion-Exchange Waveguides by Finite Difference ADI Method. *Optik* **1994**, *95*, 168–172.
31. Saarikoski, H.; Salmio, R.P.; Saarinen, J.; Eirola, T.; Tervonen, A. Fast numerical solution of nonlinear diffusion equation for the simulation of ion-exchanged micro-optics components in glass. *Opt. Commun.* **1997**, *134*, 362–370. [[CrossRef](#)]
32. Fabricius, N.; Oeste, H.; Guttman, H.; Quast, H.; Ross, L. BGG 31: A New Glass for Multimode Waveguide Fabrication. *Proc. EFOC/LAN* **1988**, *88*, 59–62.
33. Araujo, R. Colorless glasses containing ion-exchanged silver. *Appl. Opt.* **1992**, *31*, 5221–5224. [[CrossRef](#)] [[PubMed](#)]
34. Walker, R.G.; Wilkinson, C.D.W.; Wilkinson, J.A.H. Integrated optical waveguiding structures made by silver ion-exchange in glass 1: The propagation characteristics of stripe ion-exchanged waveguides: A theoretical and experimental investigation. *Appl. Opt.* **1983**, *22*, 1923–1928. [[CrossRef](#)] [[PubMed](#)]
35. Schimpf, A.; Bucci, D.; Nannini, M.; Magnaldo, A.; Couston, L.; Broquin, J.-E. Photothermal microfluidic sensor based on an integrated Young interferometer made by ion exchange in glass. *Sens. Actuators B Chem.* **2012**, *163*, 29–37. [[CrossRef](#)]
36. Onestas, L.; Bucci, D.; Ghibaudo, E.; Broquin, J.-E. Vertically Integrated Broadband Duplexer for Erbium-Doped Waveguide Amplifiers Made by Ion Exchange on Glass. *IEEE Photonics Technol. Lett.* **2011**, *23*, 648–650. [[CrossRef](#)]
37. Pantchev, B.; Danesh, P. Masking Problem in the Fabrication of Optical Waveguide Structures in Glass by Double Ion Exchange. *Jpn. J. Appl. Phys.* **1997**, *36*, 4320–4322. [[CrossRef](#)]
38. Glingener, B.B.C. Polarization Insensitive Ion-Exchanged Arrayed-Waveguide Grating Multiplexers in Glass. *Fiber Integr. Opt.* **1998**, *17*, 279–298. [[CrossRef](#)]
39. Jamon, D.; Royer, F.; Parsy, F.; Ghibaudo, E.; Broquin, J.E. Birefringence Measurements in Optical Waveguides. *J. Light. Technol.* **2013**, *31*, 3151–3157. [[CrossRef](#)]
40. Yliniemi, S.; West, B.R.; Honkanen, S. Ion-exchanged glass waveguides with low birefringence for a broad range of waveguide widths. *Appl. Opt.* **2005**, *44*, 3358–3363. [[CrossRef](#)] [[PubMed](#)]
41. Veasey, D.L.; Funk, D.S.; Sanford, N.A.; Hayden, J.S. Arrays of distributed-Bragg-reflector waveguide lasers at 1536 nm in Yb/Er codoped phosphate glass. *Appl. Phys. Lett.* **1999**, *74*, 789–791. [[CrossRef](#)]
42. Barbier, D.; Delavaux, J.M.; Kevorkian, A.; Gastaldo, P.; Jouanno, J.M. Yb/Er Integrated optics amplifiers on phosphate glass in single and double pass configurations. In Proceedings of the Optical Fiber Communication Conference, San Diego, CA, USA, 26 February 1995.
43. Josse, E.; Broquin, J.E.; Lebrasseur, E.; Fonteneau, G.; Rimet, R.; Jacquier, B.; Lucas, J. *Rare-Earth-Doped Fluoride Waveguides*; International Society for Optics and Photonics: Bellingham, WA, USA, 1997; Volume 2996, pp. 74–85.

44. Grelin, J.; Bouchard, A.; Ghibaudo, E.; Broquin, J.-E. Study of Ag⁺/Na⁺ ion-exchange diffusion on germanate glasses: Realization of single-mode waveguides at the wavelength of 1.55 μm . *Mater. Sci. Eng. B* **2008**, *149*, 190–194. [[CrossRef](#)]
45. Luo, T.; Jiang, S.; Conti, G.N.; Honkanen, S.; Mendes, S.; Peyghambarian, N. Ag/Sup⁺/Na/Sup⁺/Exchanged Channel Waveguides in Germanate Glass. *Electron. Lett.* **1998**, *34*, 2239–2240. [[CrossRef](#)]
46. Miller, S.E. Integrated Optics: An Introduction. *Bell Syst. Tech. J.* **1969**, *48*, 2059–2069. [[CrossRef](#)]
47. Voirin, G.; Rimet, R.; Chartier, G. Performances of an Ion Exchanged Star Coupler for Multimode Optical Communications. In *Optical Sciences*; Springer: Berlin/Heidelberg, Germany, 1985; Volume 48, pp. 229–231.
48. Teem Photonics. PIC Optical Waveguides for Si-Pho, Integration & Sensors. Available online: <https://www.teemphotonics.com/integrated-photonics/platform/> (accessed on 25 April 2021).
49. Hurvitz, T.; Ruschin, S.; Brooks, D.; Hurvitz, G.; Arad, E. Variable optical attenuator based on ion-exchange technology in glass. *J. Light. Technol.* **2005**, *23*, 1918–1922. [[CrossRef](#)]
50. Tervonen, A.; Honkanen, S.; Najafi, S.I. Analysis of symmetric directional couplers and asymmetric Mach-Zehnder interferometers as 1.30- and 1.55- μm dual-wavelength demultiplexers/multiplexers. *Opt. Eng.* **1993**, *32*, 2083–2091. [[CrossRef](#)]
51. Benech, P.; Persegol, D.; Andre, F.S. A glass ion exchanged Mach-Zehnder interferometer to stabilise the frequency of a laser diode. *J. Phys. D Appl. Phys.* **1990**, *23*, 617–619. [[CrossRef](#)]
52. Das, S.; Geraghty, D.F.; Peyghambarian, N. MMI splitters by ion-exchange in glass. In *Proceedings of the Integrated Optics Devices IV*; International Society for Optics and Photonics: Bellingham, WA, USA, 2000; Volume 3936, pp. 239–248.
53. Kasprzak, D.; Błahut, M.; Maciak, E. Applications of multimode interference effects in gradient waveguides produced by ion-exchange in glass. *Eur. Phys. J. Spéc. Top.* **2008**, *154*, 113–116. [[CrossRef](#)]
54. West, B.R.; Honkanen, S. MMI devices with weak guiding designed in three dimensions using a genetic algorithm. *Opt. Express* **2004**, *12*, 2716–2722. [[CrossRef](#)] [[PubMed](#)]
55. West, B.R.; Plant, D.V. Optimization of non-ideal multimode interference devices. *Opt. Commun.* **2007**, *279*, 72–78. [[CrossRef](#)]
56. Suhara, T.; Viljanen, J.; Leppihalme, M. Integrated-optic wavelength multi- and demultiplexers using a chirped grating and an ion-exchanged waveguide. *Appl. Opt.* **1982**, *21*, 2195–2198. [[CrossRef](#)] [[PubMed](#)]
57. Ruschin, S.; Hurwitz, G.; Hurwitz, T.; Kepten, A.; Arad, E.; Soreq, Y.; Eckhouse, S. Glass ion-exchange technology for wavelength management applications. *Photonics Fabr. Eur.* **2003**, *4944*, 150–159. [[CrossRef](#)]
58. Castro, J.M.; Geraghty, D.F.; West, B.R.; Honkanen, S. Fabrication and comprehensive modeling of ion-exchanged Bragg optical add-drop multiplexers. *Appl. Opt.* **2004**, *43*, 6166–6173. [[CrossRef](#)] [[PubMed](#)]
59. Casale, M.; Bucci, D.; Bastard, L.; Broquin, J.-E.; Quaranta, A. Hybrid erbium-doped DFB waveguide laser made by wafer bonding of two ion-exchanged glasses. *Ceram. Int.* **2015**, *41*, 7466–7470. [[CrossRef](#)]
60. Gardillou, F.; Bastard, L.; Broquin, J.E. Integrated optics Bragg filters made by ion exchange and wafer bonding. *Appl. Phys. Lett.* **2006**, *89*, 101123. [[CrossRef](#)]
61. Román, J.E.; Winick, K.A. Photowritten gratings in ion-exchanged glass waveguides. *Opt. Lett.* **1993**, *18*, 808–810. [[CrossRef](#)] [[PubMed](#)]
62. Montero, C.; Gomez-Reino, C.; Brebner, J.L. Planar Bragg gratings made by excimer-laser modification of ion-exchanged waveguides. *Opt. Lett.* **1999**, *24*, 1487–1489. [[CrossRef](#)] [[PubMed](#)]
63. Geraghty, D.; Provenzano, D.; Marshall, W.; Honkanen, S.; Yariv, A.; Peyghambarian, N. Gratings photowritten in ion-exchanged glass channel waveguides. *Electron. Lett.* **1999**, *35*, 585. [[CrossRef](#)]
64. Bucci, D.; Grelin, J.; Ghibaudo, E.; Broquin, J.-E. Realization of a 980-nm/1550-nm Pump-Signal (De)multiplexer Made by Ion-Exchange on Glass Using a Segmented Asymmetric Y-Junction. *IEEE Photonics Technol. Lett.* **2007**, *19*, 698–700. [[CrossRef](#)]
65. Saruwatari, M. Nd-glass laser with three-dimensional optical waveguide. *Appl. Phys. Lett.* **1974**, *24*, 603–605. [[CrossRef](#)]
66. Aoki, H.; Ishikawa, E.; Asahara, Y. Nd/Sup³⁺/Doped Glass Waveguide Amplifier at 1.054 μm . *Electron. Lett.* **1991**, *27*, 2351–2353. [[CrossRef](#)]
67. Sanford, N.A.; Malone, K.J.; Larson, D.R.; Hickernell, R.K. Y-branch waveguide glass laser and amplifier. *Opt. Lett.* **1991**, *16*, 1168–1170. [[CrossRef](#)] [[PubMed](#)]
68. Miliou, A.; Cao, X.; Srivastava, R.; Ramaswamy, R. 15-dB amplification at 1.06 μm in ion-exchanged silicate glass waveguides. *IEEE Photonics Technol. Lett.* **1993**, *5*, 416–418. [[CrossRef](#)]
69. Sanford, N.A.; Aust, J.A.; Malone, K.J.; Larson, D.R. Linewidth narrowing in an imbalanced Y-branch waveguide laser. *Opt. Lett.* **1993**, *18*, 281–283. [[CrossRef](#)] [[PubMed](#)]
70. Aust, J.A.; Malone, K.J.; Veasey, D.L.; Sanford, N.A.; Roshko, A. Passively Q-switched Nd-doped waveguide laser. *Opt. Lett.* **1994**, *19*, 1849–1851. [[CrossRef](#)]
71. Barbier, D.; Rattay, M.; Andre, F.S.; Clauss, G.; Trouillon, M.; Kevorkian, A.; Delavaux, J.M.; Murphy, E. Amplifying four-wavelength combiner, based on erbium/ytterbium-doped waveguide amplifiers and integrated splitters. *IEEE Photonics Technol. Lett.* **1997**, *9*, 315–317. [[CrossRef](#)]
72. Reichmann, K.; Iannone, P.; Birk, M.; Frigo, N.; Barbier, D.; Cassagnettes, C.; Garret, T.; Verlucco, A.; Perrier, S.; Philipsen, J. An eight-wavelength 160-km transparent metro WDM ring network featuring cascaded erbium-doped waveguide amplifiers. *IEEE Photonics Technol. Lett.* **2001**, *13*, 1130–1132. [[CrossRef](#)]
73. Patel, F.; Dicarolis, S.; Lum, P.; Venkatesh, S.; Miller, J. A Compact High-Performance Optical Waveguide Amplifier. *IEEE Photonics Technol. Lett.* **2004**, *16*, 2607–2609. [[CrossRef](#)]

74. Feuchter, T.; Mwarania, E.; Wang, J.; Reekie, L.; Wilkinson, J. Erbium-doped ion-exchanged waveguide lasers in BK-7 glass. *IEEE Photonics Technol. Lett.* **1992**, *4*, 542–544. [[CrossRef](#)]
75. Madasamy, P.; Conti, G.N.; Poyhonen, P.; Hu, Y.; Morrell, M.M.; Geraghty, D.F.; Honkanen, S.; Peyghambarian, N. Wave-guide Distributed Bragg Reflector Laser Arrays in Erbium Doped Glass Made by Dry Ag Film Ion Exchange. *Opt. Eng.* **2002**, *41*, 1084–1086.
76. Blaize, S.; Bastard, L.; Cassagnetes, C.; Broquin, J. Multiwavelengths DFB waveguide laser arrays in Yb-Er codoped phosphate glass substrate. *IEEE Photonics Technol. Lett.* **2003**, *15*, 516–518. [[CrossRef](#)]
77. Bastard, L.; Blaize, S.; Broquin, J.-E. Glass integrated optics ultranarrow linewidth distributed feedback laser matrix for dense wavelength division multiplexing applications. *Opt. Eng.* **2003**, *42*, 2800–2804. [[CrossRef](#)]
78. Arab, N.; Bastard, L.; Poëtte, J.; Broquin, J.-E.; Cabon, B. Thermal coupling impact on an MMW carrier generated using two free-running DFB lasers on glass. *Opt. Lett.* **2018**, *43*, 5500–5503. [[CrossRef](#)] [[PubMed](#)]
79. Yliniemi, S.; Honkanen, S.; Laronche, A.; Albert, J.; Ianoul, A. Photosensitivity and volume gratings in phosphate glasses for rare-earth-doped ion-exchanged optical waveguide lasers. *J. Opt. Soc. Am. B* **2006**, *23*, 2470–2478. [[CrossRef](#)]
80. Yliniemi, S.; Albert, J.; Wang, Q.; Honkanen, S. UV-exposed Bragg gratings for laser applications in silver-sodium ion-exchanged phosphate glass waveguides. *Opt. Express* **2006**, *14*, 2898–2903. [[CrossRef](#)] [[PubMed](#)]
81. Grélin, J.; Ghibaudo, E.; Broquin, J.-E. Study of deeply buried waveguides: A way towards 3D integration. *Mater. Sci. Eng. B* **2008**, *149*, 185–189. [[CrossRef](#)]
82. Bertoldi, O.; Broquin, J.E.; Vitrant, G.; Collomb, V.; Trouillon, M.; Minier, V. Use of Selectively Buried Ion-Exchange Wave-guides for the Realization of Bragg Grating Filters. In *Proceedings of the Integrated Optics and Photonic Integrated Circuits*; International Society for Optics and Photonics: Bellingham, WA, USA, 2004; Volume 5451, pp. 182–190.
83. Gardillou, F.; Bastard, L.; Broquin, J.-E. 4.25 dB gain in a hybrid silicate/phosphate glasses optical amplifier made by wafer bonding and ion-exchange techniques. *Appl. Phys. Lett.* **2004**, *85*, 5176. [[CrossRef](#)]
84. Salas-Montiel, R.; Bastard, L.; Grosa, G.; Broquin, J.-E. Hybrid Neodymium-doped passively Q-switched waveguide laser. *Mater. Sci. Eng. B* **2008**, *149*, 181–184. [[CrossRef](#)]
85. Ouslimani, H.; Bastard, L.; Broquin, J.-E. Narrow-linewidth Q-switched DBR laser on Ytterbium-doped glass. *Ceram. Int.* **2015**, *41*, 8650–8654. [[CrossRef](#)]
86. Charlet, B.; Bastard, L.; Broquin, J.E. 1 kW peak power passively Q-switched Nd(3+)-doped glass integrated waveguide laser. *Opt. Lett.* **2011**, *36*, 1987–1989. [[CrossRef](#)]
87. Charlet, B.; Bastard, L.; Broquin, J.E.; Bucci, D.; Ghibaudo, E. Supercontinuum Source Based on Ion-Exchanged Neodymium Doped Q-Switched Laser. In *Proceedings of the European Conference on Integrated Optics*, Sitges, Spain, 18–20 April 2012.
88. Legrand, L.; Bouchard, A.; Grosa, G.; Broquin, J.E. Hybrid integration of 300nm-thick LiNbO₃ films on ion-exchanged glass waveguides for efficient nonlinear integrated devices. In *Proceedings of the Integrated Optics: Devices, Materials, and Technologies XXII*; International Society for Optics and Photonics: Bellingham, WA, USA, 2018; Volume 10535, p. 105350E.
89. Macdonald, R.I.; Lam, D.K.W.; Syrett, B.A. Hybrid optoelectronic integrated circuit. *Appl. Opt.* **1987**, *26*, 842–844. [[CrossRef](#)] [[PubMed](#)]
90. Larson, D.R.; Phelan, R.J., Jr. Fast Optical Detector Deposited on Dielectric Channel Waveguides. *Opt. Eng.* **1988**, *27*, 276503. [[CrossRef](#)]
91. Larson, D.R.; Phelan, R.J. Hydrogenated amorphous germanium detectors deposited onto channel waveguides. *Opt. Lett.* **1990**, *15*, 544–546. [[CrossRef](#)] [[PubMed](#)]
92. Yi-Yan, A.; Chan, W.K.; Gmitter, T.J.; Florez, L.T.; Jackel, J.L.; Yablonovitch, E.; Bhat, R.; Harbison, J.P. Grafted GaAs Detectors on Lithium Niobate and Glass Optical Waveguides. In *Proceedings of the 5th European Conference on Integrated Optics: ECIO'89*; International Society for Optics and Photonics: Bellingham, WA, USA, 1989; Volume 1141, pp. 154–159.
93. Le Coarer, E.; Blaize, S.; Benech, P.; Stefanon, I.; Morand, A.; Léronnel, G.; Leblond, G.; Kern, P.; Fédéli, J.M.; Royer, P. Wavelength-scale stationary-wave integrated Fourier-transform spectrometry. *Nat. Photonics* **2007**, *1*, 473–478. [[CrossRef](#)]
94. Thomas, F.; De Mengin, M.; Duchemin, C.; Le Coarer, E.; Bonneville, C.; Gonthiez, T.; Morand, A.; Benech, P.; Dherbecourt, J.B.; Hardy, E.; et al. High-performance high-speed spectrum analysis of laser sources with SWIFTS technology. In *Proceedings of the Photonic Instrumentation Engineering*; International Society for Optics and Photonics: Bellingham, WA, USA, 2014; Volume 8992, p. 89920I.
95. Arnaud, L.; Bruyant, A.; Renault, M.; Hadjar, Y.; Salas-Montiel, R.; Apuzzo, A.; Léronnel, G.; Morand, A.; Benech, P.; Le Coarer, E.; et al. Waveguide-coupled nanowire as an optical antenna. *J. Opt. Soc. Am. A* **2013**, *30*, 2347–2355. [[CrossRef](#)] [[PubMed](#)]
96. High-Resolution High-Rate Laser Spectrum Analyzer. Available online: <https://resolutionspectra.com/products/zoom-spectra/> (accessed on 25 April 2021).
97. Hellesø, O.G.; Benech, P.; Rimet, R. Interferometric displacement sensor made by integrated optics on glass. *Sens. Actuators A Phys.* **1995**, *47*, 478–481. [[CrossRef](#)]
98. Lang, T.; Genon-Catalot, D.; Dandrea, P.; Duport, I.S.; Benech, P. Integrated optical displacement sensor with four quadrature phase-shifted output signals. *J. Opt.* **1998**, *29*, 135–140. [[CrossRef](#)]

99. Bastard, L.; Broquin, J.-E.; Gardillou, F.; Cassagnettes, C.; Schlotterbeck, J.P.; Rondeau, P. Development of a ion-exchanged glass integrated optics DFB laser for a LIDAR application. In Proceedings of the Integrated Optics: Devices, Materials, and Technologies XIII, San Jose, CA, USA, 26–28 January 2009; International Society for Optics and Photonics: Bellingham, WA, USA, 2009; Volume 7218, p. 721817.
100. Verbeek, M.J.; Jentink, H.W. *Optical Air Data System Flight Testing*; NLR: Amsterdam, The Netherlands, 2012.
101. Haguenaer, P.; Berger, J.-P.; Rousselet-Perraut, K.; Kern, P.; Malbet, F.; Schanen-Duport, I.; Benech, P. Integrated Optics for Astronomical Interferometry. III. Optical Validation of a Planar Optics Two-Telescope Beam Combiner. *Appl. Opt.* **2000**, *39*, 2130–2139. [[CrossRef](#)] [[PubMed](#)]
102. Berger, J.; Haguenaer, P.; Kern, P.; Perraut, K.; Malbet, F.; Schanen, I.; Severi, M.; Millan-Gabet, R.; Traub, W. Integrated Optics for Astronomical Interferometry-IV. First Measurements of Stars. *Astron. Astrophys.* **2001**, *376*, L31–L34. [[CrossRef](#)]
103. Olivier, S.; Delage, L.; Reynaud, F.; Collomb, V.; Trouillon, M.; Grelin, J.; Schanen, I.; Minier, V.; Broquin, J.E.; Ruilier, C.; et al. MAFL experiment: Development of photonic devices for a space-based multiaperture fiber-linked interferometer. *Appl. Opt.* **2007**, *46*, 834–844. [[CrossRef](#)]
104. Allenet, T.; Geoffray, F.; Bucci, D.; Canto, F.; Moisy, P.; Broquin, J.E. Microsensing of plutonium with a glass optofluidic device. *Opt. Eng.* **2019**, *58*, 060502. [[CrossRef](#)]